

## Supplemental figure legends

**Supplemental Figure 1.** Intracranial transduction of a modified pTomo lentiviral vector in the mouse hippocampus targets GFAP-positive but not NeuN-positive cells. **(A)** Stereotaxic injection of pTomo-GFP lentivirus was done to target the dentate gyrus of the mouse hippocampus and brain sections were prepared five days later. (left), Double immunofluorescence for GFP (green) and GFAP (red). (right), Double immunofluorescence for GFP (green) and NeuN (red). **(B)** Schematic representation of pTomo-H-RasV12-IRES-Cre-ER-shp53 lentiviral vector. Activation of Cre recombinase by tamoxifen results in deletion of the floxed *Id* genes exclusively in tumor cells. **(C)** High magnification microphotographs for Hematoxylin and Eosin staining and immunophenotype of the representative tumor lesion in Figure 1A. *Id-cTKO* mice were sacrificed 12 days after stereotaxic injection with Ras-V12-IRES-Cre-ER-shp53 lentivirus. Adjacent sections were immunostained using the indicated antibodies. Scale bars: 50  $\mu\text{m}$ .

**Supplemental Figure 2.** Treatment of *Id-cTKO* glioma-bearing mice with tamoxifen results in loss of expression of ID proteins and Ki67 but not H-RasV12 in glioma cells. Brain tumors from mice treated with oil or tamoxifen for four days were stained for ID2 **(A)**, ID1 **(B)** and Ki67 **(C)**. B, brain; T, tumor. **(D)** Immunostaining for H-RasV12 (red) and Id proteins (green) in mice treated with vehicle or tamoxifen and sacrificed 6 weeks after lentiviral transduction. Scale bars: 100  $\mu\text{m}$  (A,B,C); 20  $\mu\text{m}$  (D).

**Supplemental Figure 3.** The effect of ablation of *Id* genes in malignant glioma induced by Ras-V12-IRES-Cre-ER-shp53. **(A)** Expansion of glioma cells retaining ID1 and ID2 after re-growth of tamoxifen-treated Ras-V12-IRES-Cre-ER-shp53 glioma. Immunostaining for ID1 and ID2 (red) of a representative tumor lesion in mice treated with vehicle or tamoxifen and sacrificed after the

manifestation of neurological symptoms. Nuclei were counterstained with DAPI. **(B)** Double immunostaining for ID protein (red) and the stem cell marker Nestin (green) in mice treated with vehicle or tamoxifen and sacrificed 6 weeks after lentiviral transduction. **(C)** Tumor explants from advanced Ras-V12-IRES-Cre-ER-shp53 glioma generated in *Id-cTKO* mice were cultured in medium containing EGF and FGF-2 in the presence or the absence of 4-OHT for 5 days. Fixed tissues were immunostained with anti-Nestin antibody and analyzed by confocal microscopy. **(D)** Double immunostaining for ID protein (red) and the astrocytic marker GFAP (green) in mice treated with vehicle or tamoxifen and sacrificed 6 weeks after lentiviral transduction. Scale bars: 100  $\mu\text{m}$  (A); 25  $\mu\text{m}$  (insets A); 50  $\mu\text{m}$  (B,C,D).

**Supplemental Figure 4.** The expression of ID proteins in GCSs. **(A)** Immunostaining for SSEA1 (red) and ID1 (green) on a representative Ras-V12-IRES-Cre-ER-shp53 HGG in *Id-cTKO* mice. Nuclei were counterstained with DAPI (blue). **(B)** Immunostaining for SSEA1 (red) and ID2 (green) on representative Ras-V12-IRES-Cre-ER-shp53 HGG in *Id-cTKO* mice. Nuclei were counterstained with DAPI (blue). **(C)** Quantification of the fraction of SSEA1 positive cells that express ID1 or ID2 proteins. Scale bars: 20  $\mu\text{m}$ .

**Supplemental Figure 5.** Ablation of *Id* genes disrupts adhesion of GSCs to endothelial cells in the perivascular niche. **(A)** Immunostaining for ITG $\alpha$ 6 (red) and CD31 (green) on representative Ras-V12-IRES-Cre-ER-shp53 HGG in *Id-cTKO* mice treated with tamoxifen or oil. Nuclei were counterstained with DAPI (blue). Asterisks indicate the lumen of blood vessels; arrows indicate ITG $\alpha$ 6<sup>+</sup> cells within 10  $\mu\text{m}$  from CD31<sup>+</sup> cells; arrowhead indicate ITG $\alpha$ 6<sup>+</sup> cells >10  $\mu\text{m}$  from CD31<sup>+</sup> cells. **(B)** Quantification of the percentage of ITG $\alpha$ 6<sup>+</sup> cells within 10  $\mu\text{m}$  from CD31<sup>+</sup> cells.  $n = 4$  per each treatment group;  $p = 7.966\text{E-}07$ . **(C)** Immunostaining for cleaved caspase-3 on representative

Ras-V12-IRES-Cre-ER-shp53 HGG in *Id-cTKO* mice treated with tamoxifen or oil. Nuclei were counterstained with hematoxylin. **(D)** Quantification of the number of cleaved caspase-3<sup>+</sup> cells/field using a 40X objective. *n* = 3 per each treatment group. Scale bars: 20 μm (A); 200 μm (C).

**Supplemental Figure 6.** Ablation of *Id* genes does not affect expression of IL-6. **(A)** Immunostaining for IL-6 (red) on representative Ras-V12-IRES-Cre-ER-shp53 HGG in *Id-cTKO* mice treated with tamoxifen or oil. Nuclei were counterstained with DAPI. **(D)** Quantification of the fluorescence intensity for IL-6 in Ras-V12-IRES-Cre-ER-shp53 HGG in *Id-cTKO* mice treated with tamoxifen or oil. Bars indicate Mean±SD. *n* = 3 for each group. Scale bars: 50 μm.

**Supplemental Figure 7.** Constitutive EGFR signaling requires *Id* activity to maintain the transformed phenotype. **(A)** Microphotographs of *Id1L/L;Id2L/L;Id3L/L* astrocytes transformed by the expression of *EGFRvIII-Cre-ER-shp53* lentivirus (iGSCs) treated with vehicle or 4-OHT. Arrow indicates the soma of a neuron; arrowheads indicate oligodendrocytes. **(B)** Western blot analysis of cells treated as in (A) shows efficient recombination of *Id1*, *Id2* and *Id3* and induction of Rap1GAP by 4-OHT. **(C)** Cells treated as in (A) were assayed by qRT-PCR for *Id1*, *Id2* and *Id3*, *Rap1gap* and the NSC marker *nestin* along with neural lineage differentiation markers. Data represent the Mean±SD of triplicate amplification reactions. **(D)** Analysis of cleaved caspase-3 in iGSCs treated with vehicle or 4-OHT. Total cell lysates were analyzed by SDS-PAGE and immunoblotting using the indicated antibodies. Cells treated with Etoposide were used as positive control for cleaved caspase-3.  $\alpha$ -tubulin is shown as loading control. **(E)** Analysis of RAP1 activity in *Id1L/L;Id2L/L;Id3L/L* iGSCs transduced with a pLOC-GFP-RAP1AG12V;Q63E or pLOC-vector-GFP lentivirus using the RAP1 pull down assay. Protein samples were analyzed by SDS-PAGE and immunoblotting using RAP1 antibody (RAP1-GTP). Total cell lysates were analyzed by SDS-PAGE and immunoblotting using the indicated

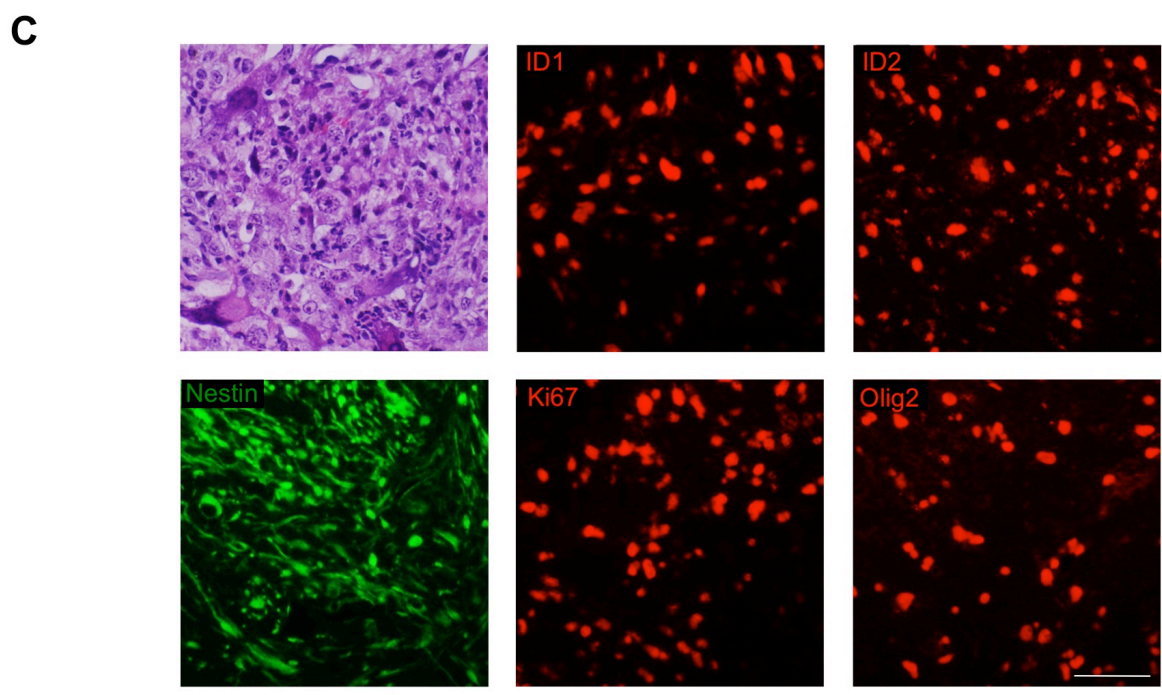
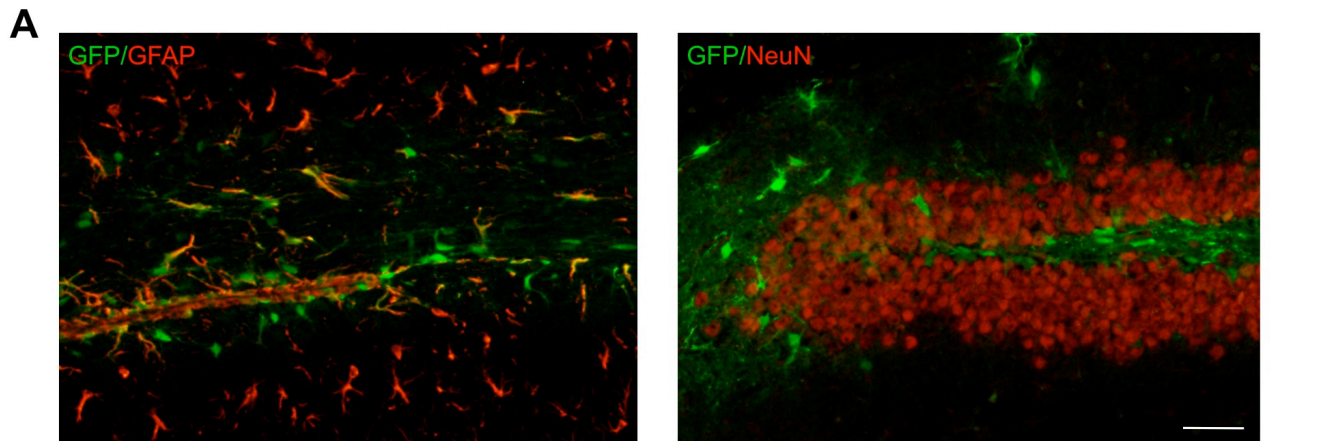
antibodies.  $\alpha$ -tubulin is shown as loading control. **(F)** Bright field microphotographs of the endothelial cell-*EGFRvIII-Cre-ER-shp53* iGSC co-cultures presented in the adhesion assay in Figure 6B. Scale bars: 200  $\mu\text{m}$  (A, upper panels); 50  $\mu\text{m}$  (A, lower panels); 100  $\mu\text{m}$  (F).

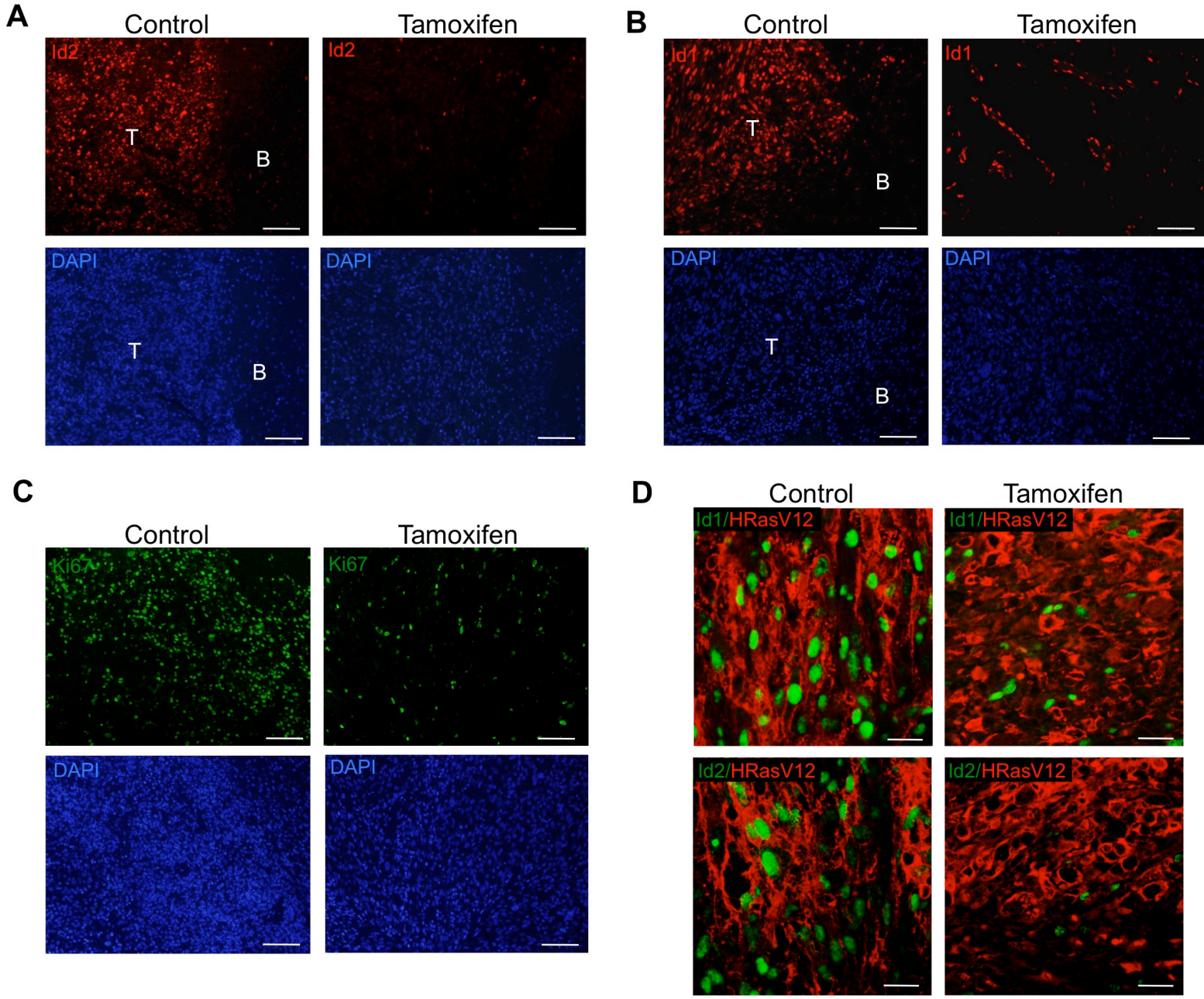
**Supplemental Figure 8.** Expression of Rap1GAP in human GICs does not affect cell proliferation **(A)** Immunostaining for BrdU in human GICs infected with pLOC-Rap1GAP-GFP, pLOC-p27<sup>KIP1</sup>-GFP or pLOC-GFP lentiviruses. **(B)** The number of BrdU<sup>+</sup> cells was determined in triplicate samples. At least 1000 cells were scored.  $p = 9.51609\text{E-}05$ . **(C)** Analysis of cleaved caspase-3 in human GICs transduced with pLOC-Rap1GAP-GFP or pLOC-GFP lentivirus. Total cell lysates were analyzed by SDS-PAGE and immunoblotting using the indicated antibodies. Cells treated with Staurosporine were used as positive control for cleaved caspase-3.  $\alpha$ -tubulin is shown as loading control. Scale bars: 200  $\mu\text{m}$ .

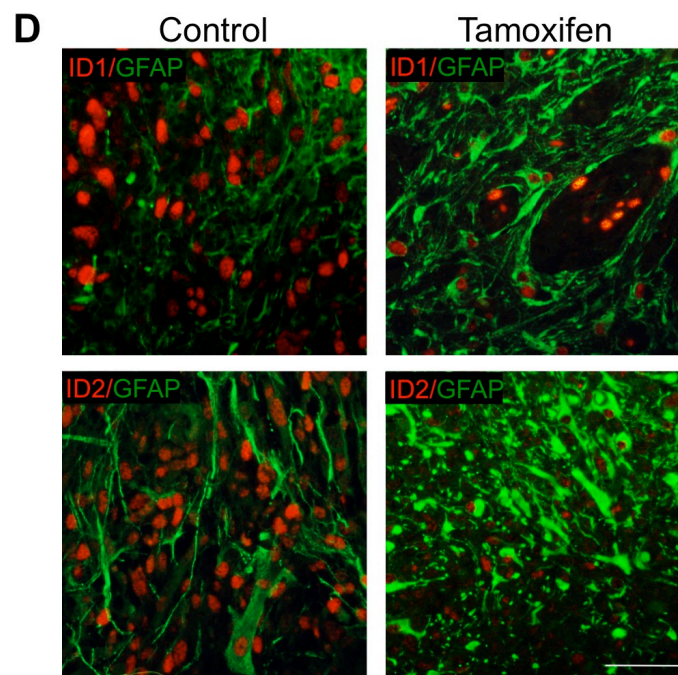
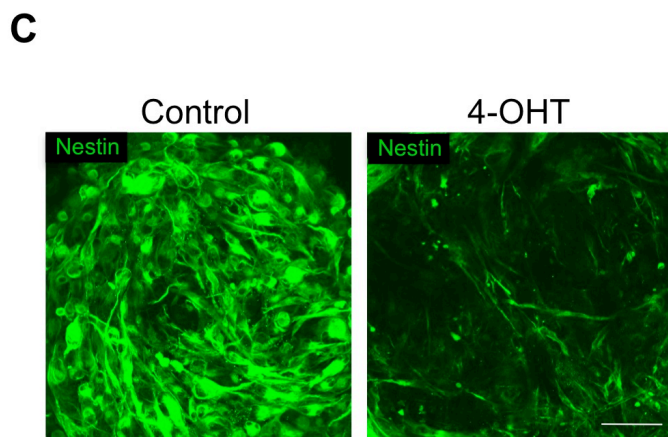
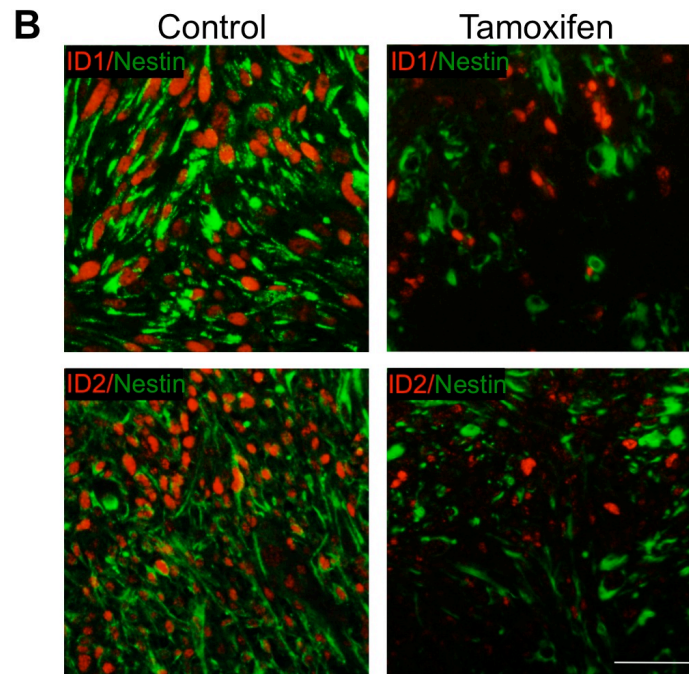
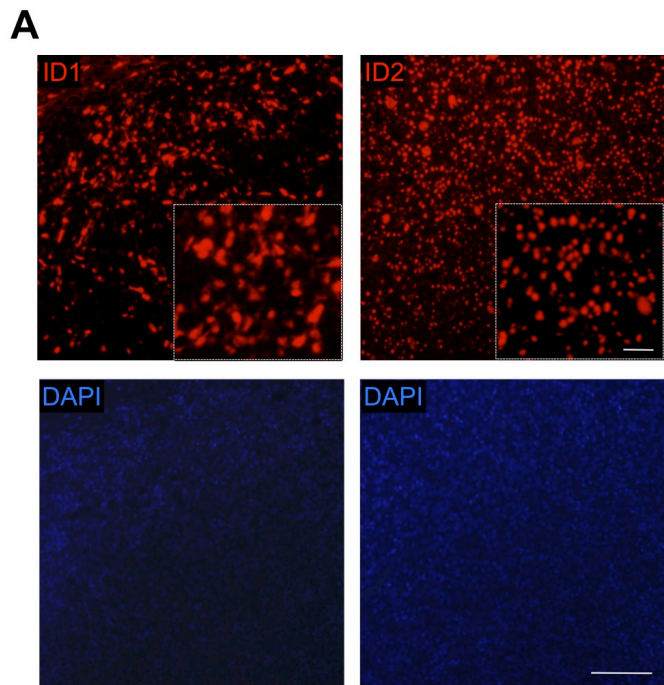
**Supplemental Figure 9.** The expression of *RAP1GAP* is reduced in human glioma. **(A)** The expression of *RAP1GAP* is significantly down regulated in 19 samples from human anaplastic astrocytoma (class 2, dark blue) compared with 23 samples from non-tumor human brain (class 1, light blue),  $p = 7.21\text{E-}9$ . **(B)** The expression of *RAP1GAP* is significantly down regulated in 45 samples from human astrocytoma (class 2, dark blue) compared with 6 samples from non-tumor human brain (temporal lobe, class 1, light blue),  $p = 5.81\text{E-}5$ . **(C)** The expression of *RAP1GAP* is significantly down regulated in 50 samples from human oligodendroglioma (class 2, dark blue) compared with 23 samples from non-tumor human brain (class 1, light blue),  $p = 1.67\text{E-}16$ .

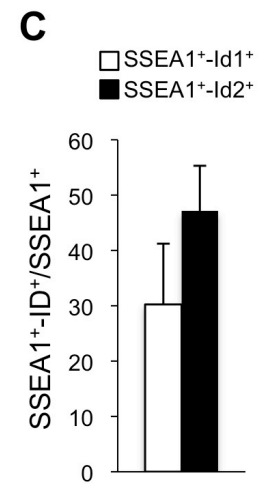
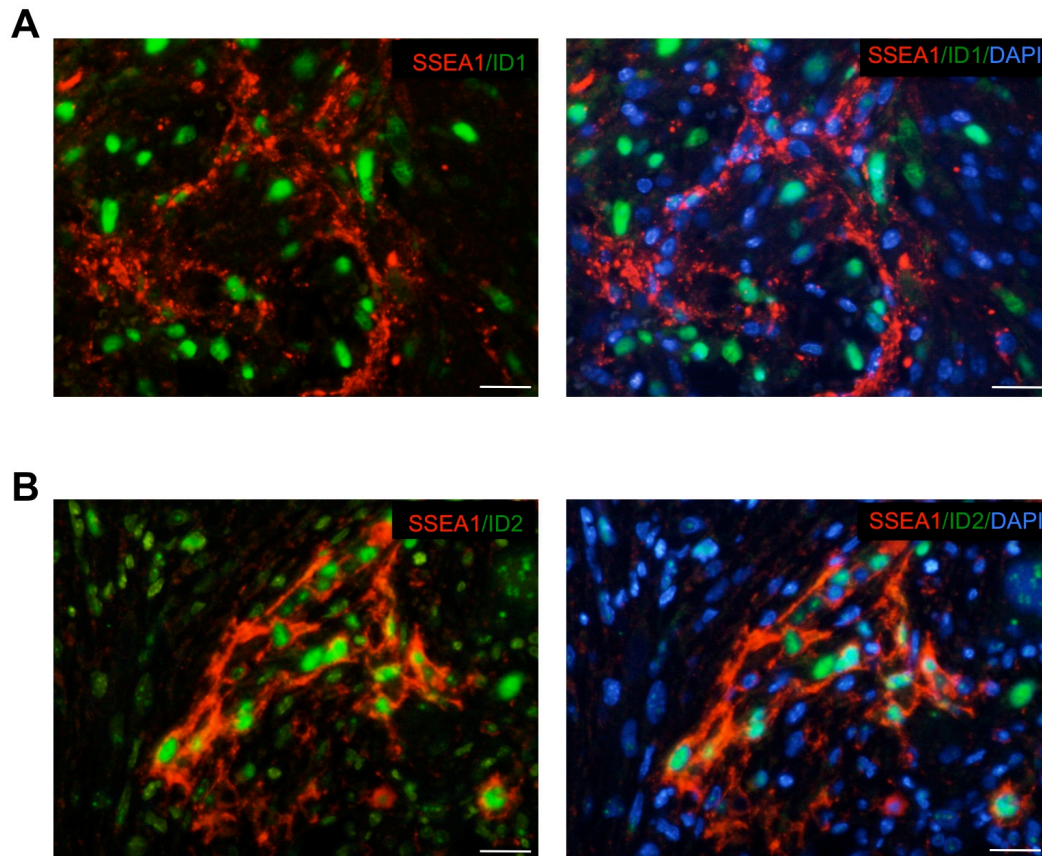
**Supplemental Figure 10.** High *ID1* expression correlates with better survival of patients within the proneural subclass of HGG. Kaplan–Meier analysis comparing survival of patients expressing high

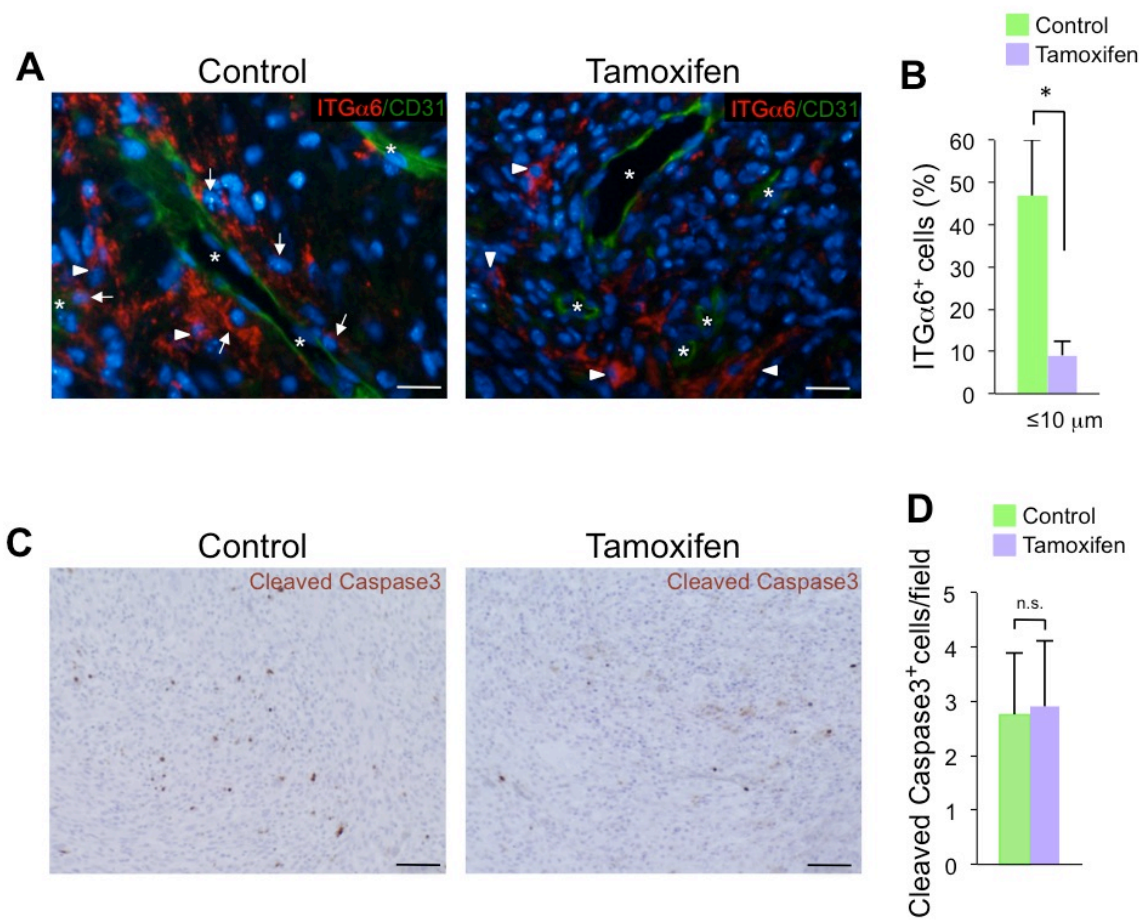
(red line) or low (blue line) levels of *ID1* in proneural (**A**), mesenchymal (**B**) or the overall (**C**) population of patients with HGG.





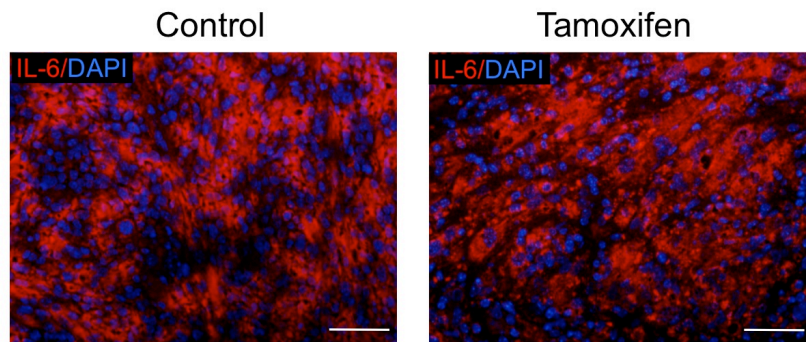




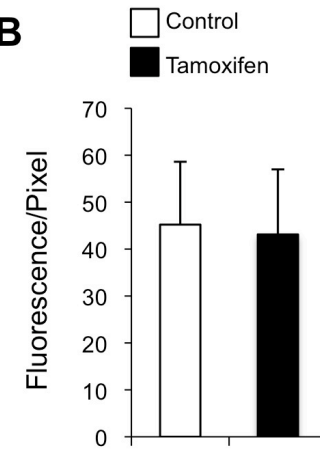


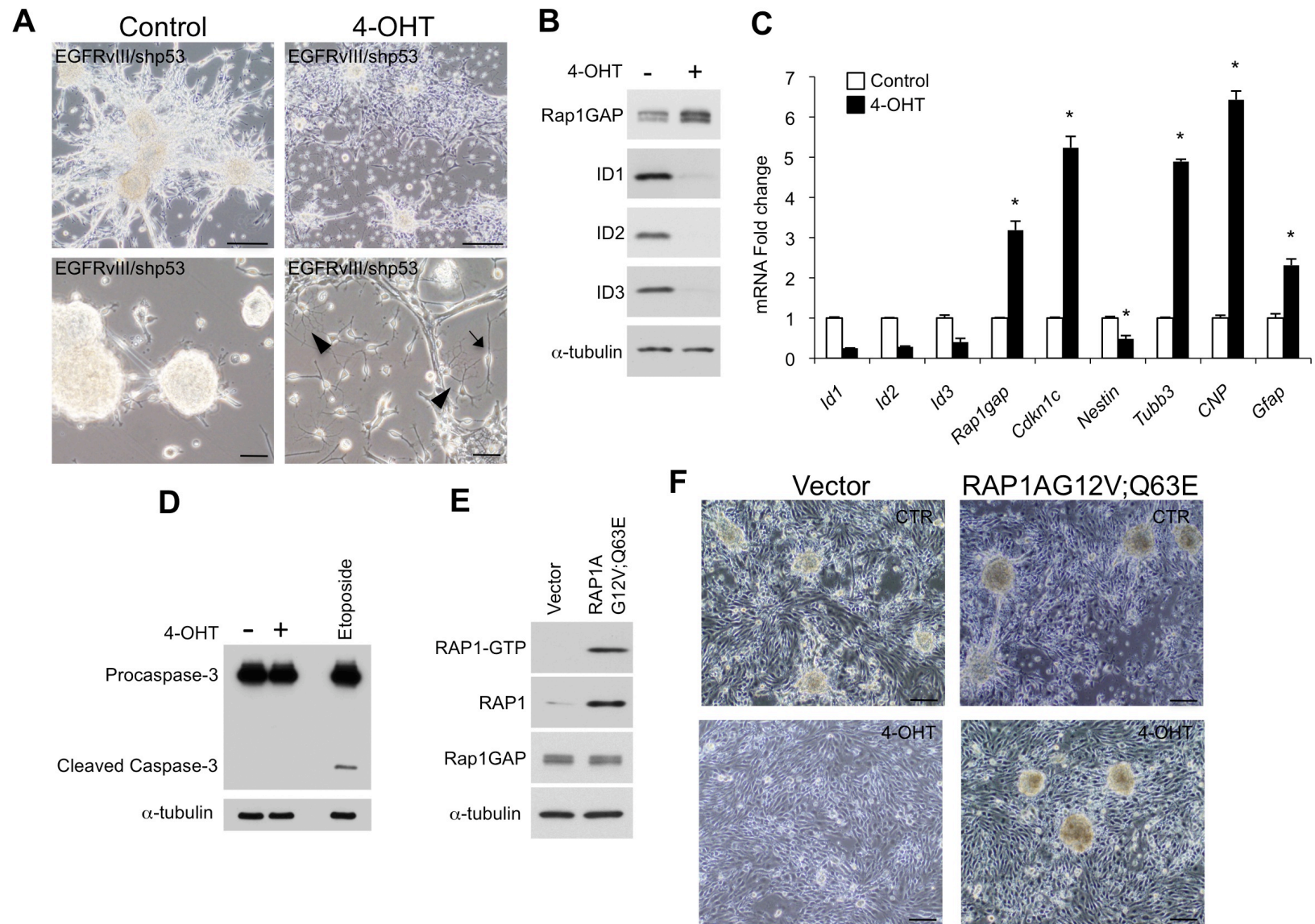
Supplemental Fig. 5

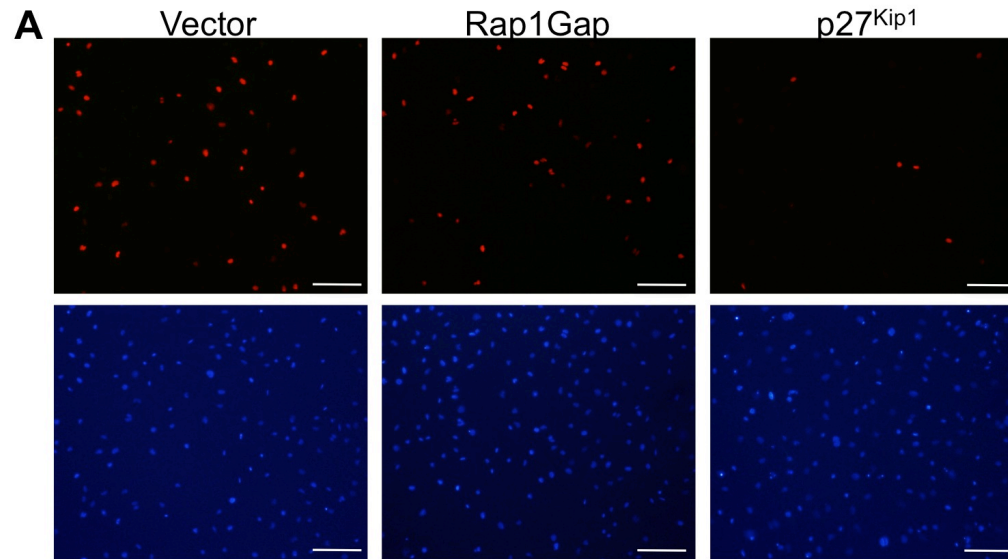
**A**



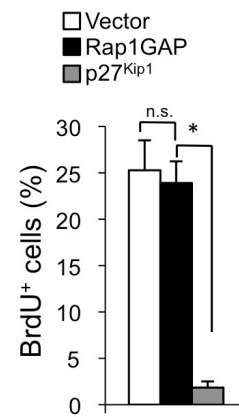
**B**



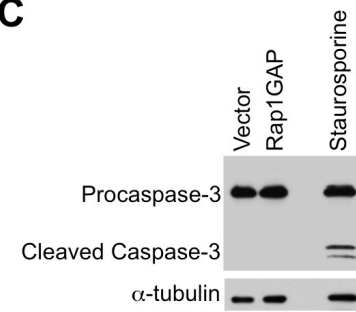




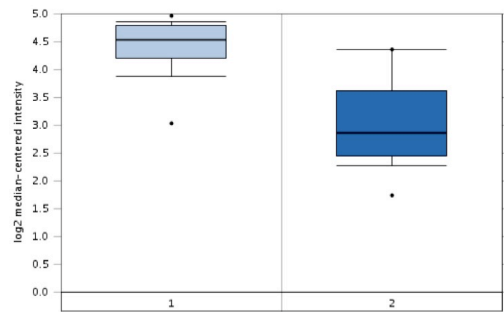
**B**



**C**

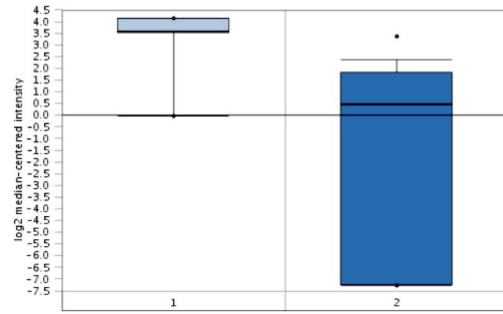


**A**



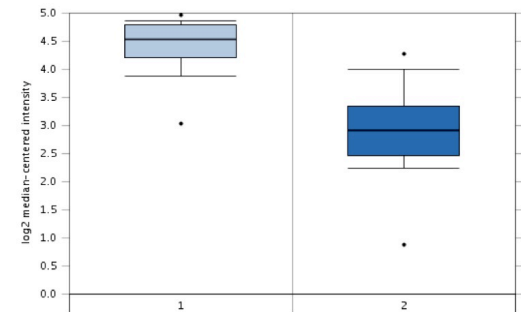
**Brain versus Anaplastic Astrocytoma**

**B**



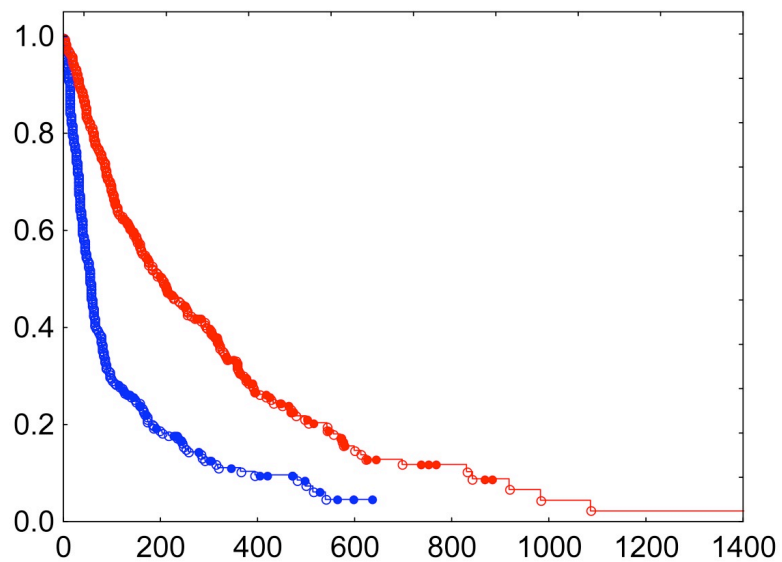
**Brain versus Astrocytoma**

**C**

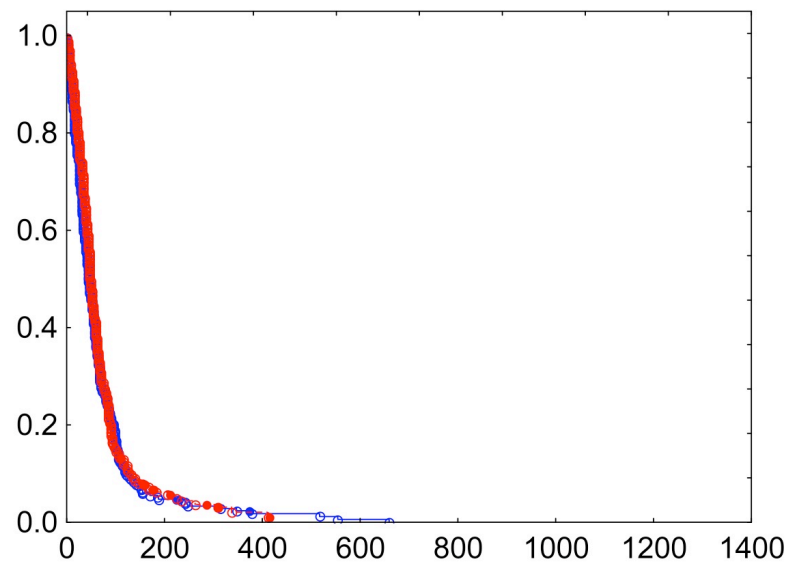


**Brain versus Oligodendroglioma**

**A** ID1 in PN samples (n=521)



**B** ID1 in MES samples (n=522)



**C** ID1 in all samples (n=1,043)

